



RESEARCH

Anatomical and radiological evaluation of frontal lobe morphometry in healthy and dementia people and machine learning-based prediction of dementia

Sağlıklı ve demanslı kişilerde frontal lob morfometrisinin anatomik ve radyolojik olarak değerlendirilmesi ve makine öğrenmesi'ne dayanan demans tahmini

Sema Polat¹, Mahmut Tunç¹, Mahmut Öksüzler², Önder Çoban³, Selma Ayşe Özel⁴, Pınar Göker¹

¹Çukurova University Faculty of Medicine, Department of Anatomy, Adana, Turkey

²Adana Medline Hospital, Department of Radiology, Adana, Turkey

³Adıyaman University Faculty of Engineering, Department of Computer Engineering, Adıyaman, Turkey

⁴Çukurova University Faculty of Engineering, Department of Computer Engineering, Adana, Turkey

Abstract

Purpose: This paper aimed to determine the morphometry of the frontal lobe and central brain region using magnetic resonance imaging in patients having dementia and healthy subjects.

Materials and Methods: 243 subjects (121 subjects having dementia; 122 subjects healthy group) aged 60-90 years over for 2 years between January 2018 and 2020 were included in this study. Also, the supervised Machine learning based (ML based) detection of dementia has been studied on this obtained real world data.

Results: The gender-related changes of frontal region measurements in dementia and healthy subjects were analyzed and, there were differences of measurements' mean values in gender. In healthy subjects, significance differences were found in all measurements (except the distance from anterior commissure to posterior commissure and outermost of corpus callosum genu to innermost of corpus callosum genu). The means of the measurements were found higher in males than in females.

Conclusions: We believe that the knowledge of our study will provide valuable reference data for our population and will help for a surgeon in planning an operation by considering measurements related to the frontal lobe. In addition, ML based supervised methods that were trained on the collected data for detection of dementia showed that it is required to provide as many attributes and instances as possible to train an accurate estimator. However, if this is not possible, by creating new features

Öz

Amaç: Bu çalışma, demanslı hastalarda ve sağlıklı bireylerde manyetik rezonans görüntüleme kullanılarak frontal lob ve merkezi beyin bölgesinin morfometrisinin belirlenmesini amaçladı.

Gereç ve Yöntem: Bu çalışmaya Ocak 2018-2020 tarihleri arasında 60-90 yaş arası 243 kişi (121 demanslı; 122 sağlıklı grup) dahil edildi. Ayrıca ortaya çıkan gerçek veriler ile denetimli Makine Öğrenmesine dayalı demans tahmini üzerinde çalışıldı.

Bulgular: Frontal bölgeyi içeren ölçümlerin cinsiyete bağlı değişimleri demans ve sağlıklı bireylerde incelendi ve ölçümlerin ortalama değerlerinde cinsiyete göre farklılıklar bulundu. Sağlıklı bireylerde bütün ölçümlerde (commissura anterior'dan commissura posterior'a olan uzaklık ölçümü ve corpus callosum genu'nun en dış kısmından corpus callosum genu'nun en iç noktasına olan mesafe ölçümleri hariç) anlamlı farklılıklar bulundu. Morfometrik ölçümlerin ortalamaları erkeklerde kadınlara göre daha yüksek bulundu.

Sonuç: Çalışmamızın, popülasyonumuz için değerli referans veriler sağlayacağına ve bir cerraha, ameliyatı planlamasında frontal lob ile ilgili ölçümlerin dikkate alınarak yardımcı olacağına inanıyoruz. Bunun yanı sıra, makine öğrenmesine dayalı denetimli öğrenme yöntemleri, demansın tespiti için toplanan veriler üzerinde doğru bir sınıflayıcı ile mümkün olduğunca fazla sayıda nitelik ve örnekleme ihtiyacı duyar. Ancak, bu mümkün değilse, nitelikler ve örneklem arasındaki gizli örüntülere dayalı yeni

Address for Correspondence: Sema Polat, Çukurova University Faculty of Medicine, Department of Anatomy, Adana, Turkey E-mail: sezaoz@hotmail.com

Received: 03.04.2023 Accepted: 25.05.2023

based on the hidden patterns between attributes and instances we could increase the success of the estimators up to 96.3% f-score value.

Keywords: Frontal lobe morphometry, anterior commissure, corpus callosum, dementia, machine learning.

niteliklerin oluşturulması ile sınıflayıcıların başarısı %96,3 f-skoru değerine kadar artırılabilir.

Anahtar kelimeler: Frontal lob morfometrisi, Commissura anterior, corpus callosum, demans, makine öğrenimi.

INTRODUCTION

Dementia is a clinical syndrome characterized by neurodegeneration and cognitive decline with a progressive deterioration of dependence. Visual ratings, volumetric and voxel-based measures of brain atrophy have demonstrated close correlations with actual atrophy, neuropathological changes, and cognitive impairment^{1,2}. And the majority of patients have an onset of dementia after age 65^{3,4}. Moreover, the incidence, and prevalence of dementia increase exponentially with age. The prevalence of dementia in those under 65 years of age is less than 5%, while in those over 85 years of age, it reaches 30-60%. Taking into account the progressive aging of the population and the expense associated with these pathologies, dementia is one of the main public health challenges in Western countries⁵. Furthermore, the prevalence of dementia is rapidly increasing in developed countries because of a significant increase in the aging population. There are several neurodegenerative diseases that cause dementia including Alzheimer's disease, and dementia with Lewy bodies. According to the 2014 World Alzheimer's Report, dementia affects approximately 44 million people worldwide, and the incidence of Alzheimer's disease (AD) is expected to triple by the year 2050^{4,6}. Specifically, AD patients show widespread atrophy, including in the medial temporal lobe (hippocampus, entorhinal cortex) and lateral temporal lobe, medial and lateral parietal lobe, and the frontal lobes, with relative sparing of the occipital lobes and sensory-motor cortex until later in the disease course⁷. The frontal lobe represents more than a third of the entire human hemisphere and the frontal lobe has a central role in cognitive functions and behaviors characteristic of adult life⁸⁻¹¹. For the evaluation of dementia, brain imaging is routinely performed and computed tomography or magnetic resonance imaging (MRI) is recommended for the diagnosis of dementia⁴. MRI could be useful to characterize a diagnosed dementia and to assess global and local atrophy. Moreover, MRI scans can also be used as outcome measures for treatments that are targeted to slow down the progression of

neurodegeneration^{12,13}. In this study, it is also studied to perform automatic detection of dementia cases by using ML techniques.

The aim of this study is to demonstrate the frontal lobe morphometry, in subjects with dementia and healthy with linear measurements using MRI, which are taken into account for the surgical anatomy for planning the procedures and preventing damage of the structures in this area. To our knowledge, there are no any studies considering frontal lobe morphometry on dementia via machine learning based prediction of dementia in the literature. Also, for this purpose, a real-world but rather small dataset of 243 instances in which each instance vector includes 11 attributes, is formed and used for training a supervised machine learning estimator to help detection of dementia.

The hypothesis of this study is that are there any relation between frontal lobe morphometric dimensions and age/gender. Also, can automatic detection of dementia cases by using ML techniques be performed.

MATERIALS AND METHODS

This study was a retrospective observational study performed in Medline Hospital Department of Radiology in Turkey. Magnetic resonance imaging was performed using a 1.5 T MRI system (Siemens; Essenza, Erlangen, Germany). The brain MRI protocol including sagittal T2-weighted spin echo (TR: 3600, TE: 87 ms; slice thickness: 5 mm; gap: 1.5 mm) was used. The measurements were performed from digital MRI images using caliper function with ×2 magnification. This study was carried out on 243 subjects (121 subjects having dementia; 122 subjects healthy group) who are appropriate for inclusion criteria, and aged 60-90 years over for 2 years between January 2018 and 2020. Moreover, unclear images having no accurate and plain reference landmarks were excluded from the study.

Some inclusion and exclusion criterias for both subjects having Dementia and healthy were stated

below.

Healthy subjects who the following criteria included in the study;

- 1) No signal abnormality and cerebral tumors, infarction, or hemorrhage on MRI.
- 2) No history of trauma on the brain
- 3) Having no surgical operation related to the brain.

Dementia subjects who the following criteria included in the study;

- 1) Patients admitted to the hospital for various reasons and diagnosed with dementia

All images were evaluated by an experienced radiologist. This study was approved by the Institutional Review Ethics Committee at Çukurova University (2021/114-62).

The measurements were made on the computer screen with an electronic caliper and estimations were expressed as millimeters. Over midsagittal view images the following measurements were performed as:

- The distance from frontal pole to anterior commissure (A)

- The distance from frontal pole to posterior commissure (B)
- The distance from frontal pole to outermost of corpus callosum genu (C)
- The distance from the frontal pole to the innermost of the corpus callosum genu (D)
- The distance from the frontal pole to the tuberculum sella (E)
- The distance from the anterior commissure to posterior commissure (F)
- The distance from frontal lobe surface to outermost of the corpus callosum genu (G)
- The distance from the frontal lobe surface to the anterior commissure (H)
- The distance from the outermost of the corpus callosum genu to the innermost of the corpus callosum genu (I) (Figure 1)

Furthermore, the data were divided also into six groups according to age: group 1; 60 – 64, group 2; 65 – 69, group 3; 70 - 74, group 4; 75 - 79, group 5; 80 - 84, group 6; 85 - 89 and the data were also analyzed according to gender.

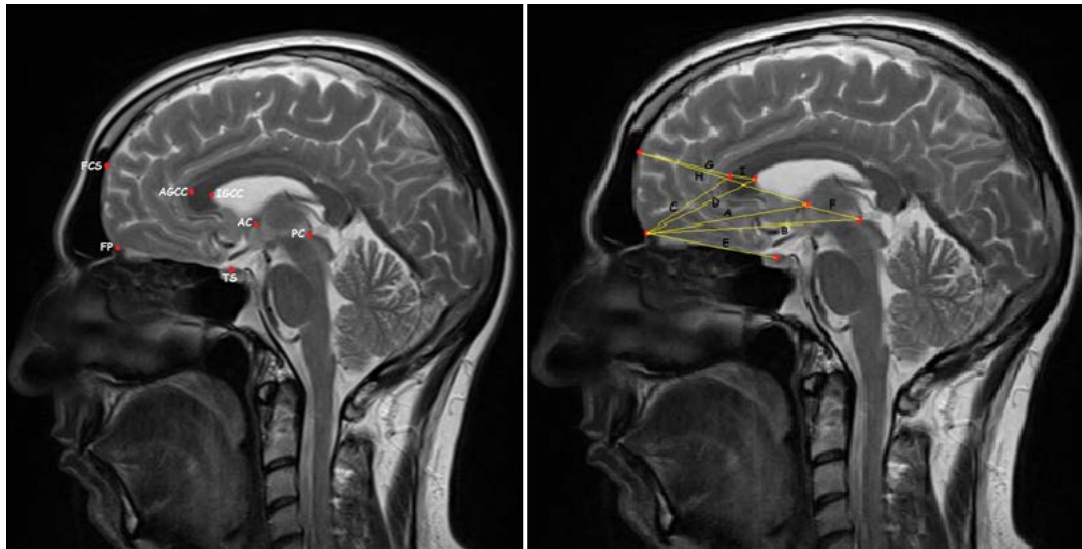


Figure 1. The midsagittal section of the brain MRI with landmarks and reference lines

Machine learning application

As a second new analysis, supervised Machine Learning techniques were applied to find the answers to research questions “Can a patient be diagnosed with dementia with frontal lobe morphometric measurements?” or “How effective are the frontal lobe morphometric measurements in diagnosing dementia?”.

Data

In this study, MRI images of 243 people were used to perform a statistical analysis of dementia cases. The analysis was performed on 9 different measurements obtained on MRI images as well as considering both gender and age information of patients.

From the machine learning (ML) perspective, this data needs to be transformed into an intermediate form to enable classifiers to run over it. Hence, first of all, we transformed the collected data of 243 patients into a 243 x 11 matrix whose rows represent patients and columns represent attributes, respectively. In the rest of the study, we refer to records of each person (i.e., each row in the data matrix) as an instance, while we refer to each of the 11 columns as an attribute (i.e., feature). Please note that one additional column representing class attribute (i.e., having dementia or nor) is also included at the rightmost side of the matrix to show the disease state of each patient. The value of 1 in this column means that the corresponding person has dementia, while the value of 2 means that the person is healthy. As our data almost includes an equal number of records (i.e., 121 dementias, 122 healthy), the data is fairly balanced across two classes. Additionally, as we have two classes (i.e., categories), our task in this study turns into a supervised binary ML task.

Machine learning methods

In this study, we used supervised ML in which training data needs to be labeled by external assistance. Supervised ML takes given data in a form of a collection of (\mathbf{x}, \mathbf{y}) pairs and tries to produce a prediction \mathbf{y}^* for a test instance \mathbf{x}^* . In this process, predictions are made via a learned mapping function $f(\mathbf{x})$ which produces an output \mathbf{y} for each input \mathbf{x} ¹⁴. The following sub-headings give a brief description of our methods used in the basic steps of supervised ML preprocessing, classification, and performance measurement and evaluation.

Preprocessing

In this step, we employed two different feature transformation (aka feature engineering) steps separately on the data to observe the effects of preprocessing on the performance of classifiers ¹⁵. These two steps are briefly described in the following sub-sections.

Encoding

The encoding task employed in this study involves basic nominal to binary conversion (both for gender and age attributes), and *discretization* (for age attribute numeric continuous value is discretized into six range groups) steps (see Table 4) on attributes to create different variants of data. This task is applied to observe the effects of feature encoding on classification performance. Also, it allows us to apply a feature selection manually. The main reason behind applying this step is that the number of features in our data is very low (i.e., only 11, see the details of our data introduced in Section 1) and feature selection algorithms often fail to select the best discriminative ones.

Partition Membership Filtering

This is another step of our preprocessing which transforms the pure data into a new form by creating new features based on existing ones ¹⁵. In this step, we used Weka’s partition membership filter^{16,17}, which transforms data into a new form by generating partition membership values. It filters instances in a way that the instances are composed of these values plus the class attribute and rendered as sparse instances ¹⁷.

This filter uses multi-instance learning (MIL), also known as multiple instance learning which is a variation of the standard supervised ML scenario¹⁸. The first study on MIL was performed to predict the drug molecule activity level ¹⁹. After that many numbers of MIL methods (e.g., diverse density, citation kNN, etc.) have been proposed and MIL has been applied to a wide spectrum of applications including image concept learning, text categorization, stock market prediction, and so on¹⁸⁻²¹ (Figure 2).

The majority of the work in MIL is concerned with binary classification problems to learn a model based on the training examples that are effective in predicting the labels of future examples as depicted in Figure 2, in traditional supervised learning, each

example is represented by a fixed-length vector of features ^{19, 22, 23}. On the other hand, in the MIL scenario, each example is represented by a multi-set (or bag) of feature vectors referred to as instances.

Classification labels are only provided for entire bags, and the task is to learn a model that is able to predict the labels for unseen bags ²⁰⁻²³.

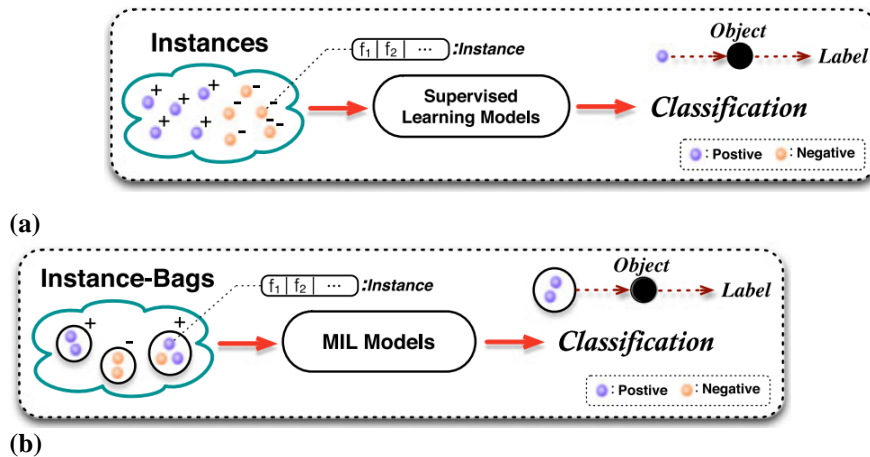


Figure 2. Traditional supervised learning scenario (a), MIL scenario (b)

In MIL problems, the instances are organized as bags of multiple instances. Let \mathbf{X} be a training set that consists of instances $\{x_1, x_2, \dots, x_n\}$ and their class labels $\{y_1, y_2, \dots, y_n\}$, where $x_i \in \mathbf{X}$ and $y_i \in \mathbf{Y}$. Formally, MIL tries to learn a model on a set of instance-bags $b = \{X_1, X_2, \dots, X_n\}$ and their labels $y = \{y_1, y_2, \dots, y_n\}$, where $X_i = \{x_{i1}, x_{i2}, \dots, x_{im}\}, \forall x_{ij} \in \mathbf{X}$ and $y_i \in \mathbf{Y}$ ^[20,23,24]. In most MIL tasks, we have $\mathbf{Y} = \{-1, +1\}$, where $y_i = -1$ or $y_i = +1$ represents a positive or negative bag b_i respectively. Two-level-classification (TLC) method is introduced in to tackle generalized MIL problems ²⁶. In the first step, each bag is converted into a single meta-instance representing the corresponding region in the instance space and has a feature/attribute for each of the discovered regions. Each attribute indicates the number of instances in the bag that can be found in the corresponding region. Together with the bag's class label, the meta-

instance can be passed to a standard propositional learner in order to learn the influence of the regions on a bag's classification (Figure 3).

This process is exemplified in Figure 3, which depicts constructing a count-based single instance from a bag with three instances and three attributes a1, a2, and a3 ²⁶. A decision tree with five nodes is used to discover regions in the instance space and the meta-instance has an attribute for each node that stands for the number of instances in the bag for that node. In this study, transforming pure data into a new form is performed by generating new features based on existing ones. For this purpose, we use Weka's Partition Membership filter which is the implementation of the TLC approach and also involves several other generators like random forest¹⁶. The reader is advised to see more details about MIL and TLC approaches^{16, 26}.

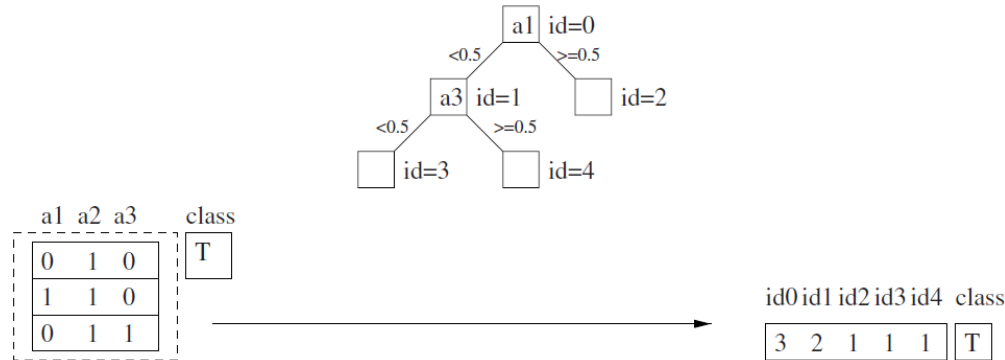


Figure 3. An example of creating a single meta-instance from a bag

Classification

In the classification stage, we used seven well-known classifiers implemented in Weka (with a version 3.8.6) ML toolkit¹⁷. The brief descriptions of the used classifiers are as follows:

NB: This is a simple probabilistic estimator, called Naïve Bayes (NB) classifier, that depends on Bayes' theory with strong independence assumptions^{27, 28}. It is easy in terms of both implementation and computation and works well on numeric and textual data when compared to other classifiers²⁷⁻²⁹.

NBM: Naïve Bayes Multinomial (NBM) classifier uses the Bayesian learning perspective and assumes that feature distributions in samples are generated by a specific parametric model^{30, 31}. In other words, NBM is a specific instance of an NB which uses a multinomial distribution for each of the features^{28, 31}.

SMO: This is the implementation of sequential minimal optimization (SMO) for training the Support Vector Machine learner in Weka^{28, 32}. SMO uses a linear kernel by default.

IBk: It is the implementation of the k-nearest neighbor classifier in Weka. It assigns each test instance to one of the predefined set of classes according to the majority class labels of the k neighbors from the training set^{28, 33}.

RF: Random Forest (RF) is an ensemble classifier of decision trees where each tree is generated by using a random vector that is sampled independently from the given input data^{28, 34}.

J48: It is an implementation of C4.5 decision tree induction algorithm. A decision tree is composed of

nodes and branches such that each node and branch represent an attribute and a value that a node can take respectively^{28, 35, 36}. Classification of a new instance is done by starting the root node, and following the matching branches until a leaf node, which represents a class label, is reached.

RT: Random Tree (RT) classifier constructs a decision tree that considers K randomly chosen attributes at each node. It does not perform pruning and also has an option to allow the estimation of class probabilities based on a hold-out set^{17, 34}.

The mathematical definitions of these methods are not given in this paper to save space and reduce the complexity of the study. Nevertheless, the reader is advised to see more details on these classifiers^{17, 28}.

Performance Measurement and Evaluation

Since we have two target class labels in our data, we performed supervised binary ML tasks using classifiers. To measure the performance of a classifier in a binary classification task, actual and predicted labels of test instances are grouped into four main categories that are TP (True Positives), TN (True Negatives), FP (False Positives), and FN (False Negatives) to derive a confusion matrix^{28, 37}. Using the number of instances in these four categories, several well-known evaluation metrics can be computed. In this study, the performance measure of estimators is performed by using the f1-score (or f-measure) which is formulated as follows³⁷:

$$f1 - score = \frac{2 \times P \times R}{P + R}$$

where $P = TP/(TP + FP)$ and $R = TP/(TP + FN)$. Model evaluation is on the other hand often performed by dividing the dataset into two disjoint subsets namely, training and test sets. In this study, we use k-fold cross-validation to evaluate our learning models (or estimators) ³⁸. In this way of evaluation, the data at hand is divided into k equal-sized subsets each of which is picked as a test set and the remaining $k - 1$ subsets taken as a training set^{28, 37}. Then, the average of the f1-scores is computed. Note that we configured our models to run with 10-fold cross-validation in this study.

Statistical analysis

Statistical analysis of the study data was performed using Statistical Package for the Social Sciences (SPSS) version 21.0 software for Windows. Normality assumption was decided to Shapiro Wilk test. From these measurements, means, standard deviations (SD), minimum (min.) and maximum (max.) values were calculated. In all statistical analyses; p value under 0.05 was considered to be statistically significant. According to Shapiro Wilk test result, ANOVA was used to the comparison of groups according to gender and ages.

RESULTS

The values of minimum, maximum, mean, and standard deviations of the measurements in 243 subjects (121 dementia and 122 healthy groups) were shown in Table 1. Distance from the frontal pole to the anterior commissure is 54.38 ± 3.07 mm; from the frontal pole to posterior commissure 80.29 ± 4.09 mm; from frontal pole to outermost of corpus callosum genu 34.73 ± 2.83 mm; from frontal pole to innermost of corpus callosum genu 41.95 ± 3.25 mm; from frontal pole to tuberculum sella 49.95 ± 3.84 mm; from anterior commissure to posterior commissure 25.72 ± 1.82 mm; from frontal lobe surface to outermost of corpus callosum genu 32.36 ± 2.71 mm; from frontal lobe surface to anterior commissure 58.93 ± 3.33 mm; from outermost of corpus callosum genu to innermost corpus callosum genu 7.87 ± 1.74 mm in healthy subjects and the same values were as 53.95 ± 3.60 mm, 81.01 ± 3.98 mm, 34.76 ± 2.81 mm, 42.12 ± 3.31 mm, 49.99 ± 3.35 mm, 25.38 ± 3.66 mm, 32.90 ± 2.89 mm, 58.43 ± 3.51 mm, 7.70 ± 1.81 mm respectively in people with dementia. According to these results, the difference was found in the distance from anterior commissure to posterior commissure (F) between two groups ($p < 0.05$). Some

measurement results were higher in healthy group than in dementia subjects (A, H, and I), whereas B, C, D, F, and G parameters were lower in healthy groups than dementia subjects. Also, only one parameter (E) of dementia subjects were similar to healthy subjects (Table 1). Also, age-related changes of frontal lobe and central region of brain measurements (mm) in dementia subjects and healthy group subjects were shown in Table 2. According to these results, there were significant differences in all measurements in dementia subjects, whereas significant differences were found in C, D, G, H and I parameters in healthy subjects. D, E, F, and I parameters were highest in the first decade and lowest in six decades. C, G, and H values were highest in the second decade and C, G were lowest in six decades, H value was lowest in the fifth decade. Also, a parameter took the highest value in third decade and lowest value in the fifth decade in dementia subjects. Additionally, in healthy subjects, A, B, G, and I parameters' the highest and the lowest values were in decades 1, and 6, respectively. Also, D, and E parameters were lowest in six decades, C, and H were lowest in the fifth decade. Moreover, D, and E measurements took the highest value in the second and the third decades, respectively. C and H values were highest in fourth and first decades, respectively. F measurement was highest in second decade lowest in fourth decade (Table 2). Additionally, when we analyzed the gender-related changes of these measurements (mm) in dementia and healthy subjects, there were differences in measurements mean values among gender. In healthy subjects, a significant difference was found in all measurements (except F and I parameters). Moreover, there were significant differences in C, D, G, and H parameters in dementia subjects ($p < 0.05$). The means of the measurements were found higher in males than in females (Table 3).

In this section, we present the results of our extensive experiments on our data using different ML methods briefly introduced in Section 2.2. Please note that we employed the methods with the help of the Weka software (with version 3.8.6) which is an ML toolkit written in Java programming language. Hence, we first structured our data matrix to be in ARFF (Attribute Relation File Format) in 12 different ways (DS01 through DS12) which are summarized in Table 4. As seen in Table 4, the first six datasets (DS01 up to DS06) include gender and age attributes in nominal or binary types, while the other datasets exclude either gender or age or both (i.e., DS12)

attributes. The reason behind creating these different datasets is to explore the effects of different attribute types on the performance of classifiers. In the experimental phase, we used all classifiers and filters with default parameter settings and configured classifiers to run with 10-fold cross-validation. In the first step, we performed classification experiments to automatically predict whether a person is healthy or not. Using the twelve variants of the data (see Table 4) and well-known classifiers, we obtained f1-scores as given in Table 5. In Table 5, the best f1 score value for each dataset is written in bold, and the best classification f1 score for the table is written in red. As seen in Table 5, classifiers produce slightly

different results, and the accuracy of automatically predicting the health status of a person ranges from 0.504 to 0.625. These results show that using the originally obtained 11 features, it is not possible to achieve satisfying results for this task. In detail, the worst results are produced by the NB classifier, while the best ones are often obtained by the RF classifier. Creating different variants of the data has also an effect on the results and the highest result (i.e., 0.625) is obtained by the NBM classifier on the DS09 variant that does not include the gender information but includes age-group information in binary format (i.e., one-hot-encoding).

Table 1. The means, standard deviations, and ranges of the measurements (mm) in dementia subjects and healthy group subjects with magnetic resonance imaging

Groups	Measurements	Number	Mean	SD	Min.	Max.	P value for groups
Dementia	A	121	53.95	3.60	43.00	62.00	0.313
Healthy group	A	122	54.38	3.07	46.00	61.00	
Dementia	B	121	81.01	3.98	71.00	93.00	0.185
Healthy group	B	122	80.29	4.09	70.00	91.00	
Dementia	C	121	34.76	2.81	27.00	42.00	0.932
Healthy group	C	122	34.73	2.83	29.00	43.00	
Dementia	D	121	42.12	3.31	33.00	52.00	0.696
Healthy group	D	122	41.95	3.25	35.00	51.00	
Dementia	E	121	49.99	3.35	41.00	61.00	0.944
Healthy group	E	122	49.95	3.84	39.00	60.00	
Dementia	F	121	27.38	3.66	21.00	42.00	<0.001
Healthy group	F	122	25.72	1.82	21.00	30.00	
Dementia	G	121	32.90	2.89	23.00	42.00	0.135
Healthy group	G	122	32.36	2.71	27.00	40.00	
Dementia	H	121	58.43	3.51	51.00	66.00	0.260
Healthy group	H	122	58.93	3.33	48.00	68.00	
Dementia	I	121	7.70	1.81	4.00	14.00	0.446
Healthy group	I	122	7.87	1.74	4.00	12.00	

A: The distance from frontal pole to anterior commissure; B: The distance from the frontal pole to the posterior commissure; C: The distance from the frontal pole to the outermost of the corpus callosum genu; D: The distance from the frontal pole to the innermost of the corpus callosum genu; E: The distance from frontal pole to tuberculum sella; F: The distance from the anterior commissure to the posterior commissure; G: The distance from the frontal lobe surface to the outermost of the corpus callosum genu; H: The distance from the frontal lobe surface to anterior commissure; I: The distance from outermost of corpus callosum genu to the innermost of the corpus callosum genu; SD: Standard deviation; Min.: Minimum; Max.: Maximum

Table 2. Age related changes of frontal lobe and central region of brain measurements (mm) in dementia subjects and healthy group subjects with magnetic resonance imaging

Measurements	Decades	Dementia group n=121	Mean	SD	P	Healthy group n=122	Mean	SD	P
A	1 (60-64 years)	15	51.93	4.83	<0.001	20	55.30	2.74	0.530
	2 (65-69 years)	25	55.40	2.40		22	55.05	2.73	

	3 (70-74 years)	18	56.00	2.97		28	54.89	3.01	
	4 (75-79 years)	23	54.70	2.69		13	54.62	2.47	
	5 (80-84 years)	26	52.42	3.16		29	53.28	3.12	
	6 (85-89 years)	14	52.50	4.35		10	52.60	4.17	
B	1 (60-64 years)	15	83.00	4.34	<0.001	20	55.30	4.05	0.480
	2 (65-69 years)	25	82.32	3.21		22	55.05	3.83	
	3 (70-74 years)	18	82.05	3.44		28	54.89	4.05	
	4 (75-79 years)	23	81.56	3.15		13	54.62	3.49	
	5 (80-84 years)	26	78.96	3.78		29	53.28	4.04	
	6 (85-89 years)	14	78.14	4.49		10	52.60	4.52	
C	1 (60-64 years)	15	35.47	2.50	0.041	20	35.10	2.45	0.029
	2 (65-69 years)	25	35.52	2.68		22	35.00	2.85	
	3 (70-74 years)	18	35.00	3.48		28	35.50	2.70	
	4 (75-79 years)	23	35.39	2.46		13	35.85	3.18	
	5 (80-84 years)	26	33.73	2.38		29	33.45	2.49	
	6 (85-89 years)	14	33.29	3.07		10	33.60	3.27	
D	1 (60-64 years)	15	44.13	2.77	<0.001	20	43.45	2.95	<0.001
	2 (65-69 years)	25	43.84	2.79		22	43.46	2.91	
	3 (70-74 years)	18	43.00	3.20		28	42.79	2.83	
	4 (75-79 years)	23	42.09	2.47		13	42.31	2.78	
	5 (80-84 years)	26	40.12	2.93		29	39.83	2.84	
	6 (85-89 years)	14	39.57	3.46		10	39.10	2.92	
E	1 (60-64 years)	15	51.07	2.87	0.044	20	50.50	3.72	0.248
	2 (65-69 years)	25	50.92	3.42		22	50.00	4.12	
	3 (70-74 years)	18	49.83	3.40		28	50.96	2.85	
	4 (75-79 years)	23	50.74	3.66		13	49.92	3.50	
	5 (80-84 years)	26	48.81	3.21		29	49.41	4.48	
	6 (85-89 years)	14	48.36	2.47		10	47.60	4.01	

F	1 (60-64 years)	15	30.20	5.35	0.008	20	25.70	2.18	0.540
	2 (65-69 years)	25	27.88	2.98		22	25.77	1.88	
	3 (70-74 years)	18	26.72	2.52		28	26.29	1.76	
	4 (75-79 years)	23	27.74	4.01		13	25.39	1.76	
	5 (80-84 years)	26	26.08	3.14		29	25.41	1.66	
	6 (85-89 years)	14	26.14	2.63		10	25.50	1.72	
G	1 (60-64 years)	15	33.73	3.15	0.016	20	33.85	3.05	<0.001
	2 (65-69 years)	25	33.80	2.24		22	33.50	2.43	
	3 (70-74 years)	18	33.72	3.25		28	32.64	2.63	
	4 (75-79 years)	23	33.04	2.71		13	32.08	2.40	
	5 (80-84 years)	26	31.65	2.08		29	30.86	2.05	
	6 (85-89 years)	14	31.43	3.78		10	30.80	2.44	
H	1 (60-64 years)	15	58.20	3.88	0.006	20	60.90	3.14	0.006
	2 (65-69 years)	25	59.80	3.10		22	59.96	2.34	
	3 (70-74 years)	18	59.33	3.11		28	58.57	3.62	
	4 (75-79 years)	23	59.30	3.50		13	56.92	3.15	
	5 (80-84 years)	26	56.50	3.39		29	58.17	3.31	
	6 (85-89 years)	14	57.29	3.12		10	58.60	3.20	
I	1 (60-64 years)	15	8.73	2.12	<0.001	20	9.50	1.36	<0.001
	2 (65-69 years)	25	8.64	1.47		22	9.14	1.21	
	3 (70-74 years)	18	8.28	1.78		28	8.07	1.46	
	4 (75-79 years)	23	7.44	1.75		13	7.00	1.47	
	5 (80-84 years)	26	6.58	1.50		29	6.59	0.95	
	6 (85-89 years)	14	6.71	0.99		10	6.20	1.40	

A: The distance from frontal pole to anterior commissure; B: The distance from frontal pole to posterior commissure; C: The distance from frontal pole to outermost of corpus callosum genu; D: The distance from frontal pole to innermost of corpus callosum genu; E: The distance from frontal pole to tuberculum sellae; F: The distance from anterior commissure to posterior commissure; G: The distance from frontal lobe surface to outermost of corpus callosum genu; H: The distance from frontal lobe surface to anterior commissure; I: The distance from outermost of corpus callosum genu to innermost of corpus callosum genu; SD: Standard deviation; Min.: Minimum; Max.: Maximum

Table 3. Gender related changes of frontal lobe and central region of brain measurements (mm) in dementia subjects and healthy group subjects with magnetic resonance imaging

Measurement/Gender	Healthy group n=122				Dementia Group n=121			
		Mean	SD		Mean	SD		
A	Male	55	55.40	2.97	Male	60	54.50	3.27
	Female	67	53.55	2.93	Female	61	53.41	3.87
	Total	122	54.39	3.08	Total	121	53.95	3.61
p value	0.001				0.097			
B	Male	55	81.33	4.16	Male	60	81.55	3.44
	Female	67	79.45	3.88	Female	61	80.49	4.42
	Total	122	80.30	4.10	Total	121	81.02	3.98
p value	0.011				0.145			
C	Male	55	35.58	2.85	Male	60	35.38	2.85
	Female	67	34.04	2.64	Female	61	34.16	2.67
	Total	122	34.74	2.83	Total	121	34.77	2.82
p value	0.03				0.017			
D	Male	55	43.16	3.15	Male	60	42.87	3.06
	Female	67	40.97	3.02	Female	61	41.39	3.41
	Total	122	41.96	3.26	Total	121	42.12	3.31
p value	<0.001				0.014			
E	Male	55	50.85	3.67	Male	60	50.50	3.63
	Female	67	49.22	3.85	Female	61	49.49	3.00
	Total	122	49.96	3.84	Total	121	49.99	3.35
p value	0.019				0.098			
F	Male	55	25.91	1.64	Male	60	27.63	3.43
	Female	67	25.58	1.96	Female	61	27.13	3.90
	Total	122	25.73	1.82	Total	121	27.38	3.67
p value	0.326				0.453			
G	Male	55	33.20	2.95	Male	60	33.68	2.80
	Female	67	31.67	2.31	Female	61	32.13	2.80
	Total	122	32.36	2.72	Total	121	32.90	2.90
p value	0.002				0.003			
H	Male	55	59.71	3.22	Male	60	59.27	3.41
	Female	67	58.30	3.32	Female	61	57.62	3.45
	Total	122	58.93	3.34	Total	121	58.44	3.51
p value	0.020				0.010			
I	Male	55	8.09	1.59	Male	60	7.80	1.73
	Female	67	7.70	1.85	Female	61	7.61	1.91
	Total	122	7.88	1.74	Total	121	7.70	1.82
p value	0.221				0.561			

A: The distance from the frontal pole to the anterior commissure; B: The distance from the frontal pole to the posterior commissure; C: The distance from the frontal pole to the outermost of the corpus callosum genu; D: The distance from the frontal pole to the innermost of corpus callosum genu; E: The distance from the frontal pole to the tuberculum sellae; F: The distance from the anterior commissure to the posterior commissure; G: The distance from frontal lobe surface to outermost of corpus callosum genu; H: The distance from the frontal lobe surface to the anterior commissure; I: The distance from the outermost of the corpus callosum genu to the innermost of corpus callosum genu; SD: Standard deviation; Min.: Minimum; Max.: Maximum

Table 4. Different types of datasets created from the data matrix considering the inclusion, exclusion, and nominal-binary conversion statuses of gender and age attributes

Dataset	# of ...			Nominal/Binary Attributes	
	instances	attributes	classes	Gender	Age
DS01	243	11	2	Nominal {M, F}	Numeric {60-89}
DS02	243	11	2	Binary {0, 1}	Numeric {60-89}
DS03	243	11	2	Nominal {M, F}	Nominal {G1, G2, G3, G4, G5, G6}
DS04	243	16	2	Nominal {M, F}	Binary {G1: {0, 1}, G2: {0, 1}, G3: {0, 1}, G4: {0, 1}, G5: {0, 1}, G6: {0, 1}}
DS05	243	11	2	Binary {0, 1}	Nominal {G1, G2, G3, G4, G5, G6}
DS06	243	16	2	Binary {0, 1}	Binary (the same as DS4)
DS07	243	10	2	Nominal {M, F}	Excluded
DS08	243	10	2	Binary {0, 1}	Excluded
DS09	243	15	2	Excluded	Binary (the same as DS4)
DS10	243	10	2	Excluded	Nominal {G1, G2, G3, G4, G5, G6}
DS11	243	10	2	Excluded	Numeric {60-89}
DS12	243	9	2	Excluded	Excluded

Table 5. Obtained f1 scores of well-known classifiers considering different variants of the data

Dataset	Classifier						
	NB	NBM	SMO	IBk	J48	RF	RT
DS01	0.523	NA	0.553	0.551	0.555	0.605	0.600
DS02	0.514	0.561	0.553	0.551	0.555	0.584	0.539
DS03	0.511	NA	0.588	0.550	0.613	0.580	0.523
DS04	0.525	NA	0.588	0.550	0.593	0.580	0.531
DS05	0.510	NA	0.588	0.550	0.613	0.576	0.556
DS06	0.525	0.613	0.588	0.550	0.593	0.572	0.580
DS07	0.511	NA	0.557	0.556	0.560	0.617	0.588
DS08	0.519	0.568	0.557	0.556	0.560	0.593	0.527
DS09	0.515	0.625	0.588	0.513	0.572	0.593	0.547
DS10	0.504	NA	0.588	0.513	0.572	0.580	0.560
DS11	0.523	0.568	0.535	0.559	0.530	0.609	0.555
DS12	0.519	0.579	0.551	0.584	0.542	0.601	0.593

Please notice that the NA value under the column NBM means that the classifier was not run since the NBM estimator cannot handle datasets including categorical or nominal attribute values. These results show that the NBM classifier is more suitable for datasets if they do not include nominal attributes. On the data variants including nominal attributes, RF often seems to be a better option but J48 is also another alternative classifier that is superior to other ones. Excluding both gender and age information causes to decrease in classification accuracy, but considering the highest result (i.e., 0.625) on the DS09 shows that gender information does not help to discriminate instances when age information is included as a binary encoding of group information.

As our results are not satisfying, we tried to improve the performance of the estimators to enable a scenario such that an ML model assists medical personnel while they reach a decision about a dementia case. In this case, one of the possible solutions is to use feature selection that selects the best discriminative features. However, this option did not improve our results, since the number of features in our data is already very low. Hence, we have focused on creating new features based on the membership information of existing ones in a supervised manner. Based on our experimental evaluations (not reported here to save space), we decided to use the partition membership filter

introduced in Section 2.1 with the help of Weka’s “Partition Membership” filter.

In the second phase of our experiments, therefore, we first passed the data through the partition membership filter and then performed classification experiments on the transformed data that is composed of newly generated attribute values based on their membership to the detected partitions or

regions. In this second step, we have employed the filter by using three different partition generators (i.e., J48, RF, and RT) that are also employed as an estimator in the classification step. Table 6 presents the results of this second step considering different estimators and variants of the data in a way such that the columns P and F represent the partition generator and the number of newly generated features respectively.

Table 6. Obtained fl scores under different circumstances where estimator, partition generator, and data variant are different

Dataset	P	F	Classifier						
			NB	NBM	SMO	IBk	J48	RF	RT
DS01	J48	29	0.622	0.608	0.719	0.719	0.707	0.719	0.719
	RF	10254	0.807	0.827	0.897	0.716	0.712	0.782	0.654
	RT	145	0.736	0.774	0.889	0.893	0.877	0.889	0.926
DS02	J48	29	0.622	0.608	0.719	0.719	0.707	0.719	0.719
	RF	10142	0.770	0.807	0.926	0.708	0.720	0.774	0.671
	RT	153	0.761	0.827	0.901	0.889	0.844	0.901	0.914
DS03	J48	75	0.675	0.712	0.864	0.872	0.827	0.868	0.881
	RF	11170	0.720	0.724	0.881	0.724	0.683	0.745	0.641
	RT	175	0.699	0.765	0.835	0.840	0.778	0.848	0.852
DS04	J48	77	0.749	0.765	0.893	0.905	0.844	0.897	0.905
	RF	10846	0.802	0.823	0.901	0.716	0.670	0.774	0.679
	RT	169	0.683	0.753	0.856	0.864	0.782	0.864	0.889
DS05	J48	75	0.675	0.712	0.864	0.872	0.827	0.868	0.881
	RF	11396	0.720	0.732	0.860	0.712	0.654	0.757	0.700
	RT	165	0.728	0.773	0.881	0.872	0.831	0.868	0.897
DS06	J48	77	0.749	0.765	0.893	0.905	0.844	0.897	0.905
	RF	10894	0.790	0.794	0.848	0.736	0.733	0.778	0.621
	RT	173	0.677	0.778	0.885	0.877	0.818	0.889	0.885
DS07	J48	29	0.622	0.608	0.719	0.719	0.707	0.719	0.719
	RF	10594	0.786	0.819	0.885	0.728	0.658	0.807	0.654
	RT	145	0.710	0.790	0.930	0.926	0.823	0.934	0.934
DS08	J48	29	0.622	0.608	0.719	0.719	0.707	0.719	0.719
	RF	10502	0.782	0.811	0.877	0.724	0.674	0.802	0.671
	RT	141	0.732	0.823	0.914	0.914	0.848	0.914	0.938
DS09	J48	63	0.757	0.774	0.851	0.863	0.801	0.851	0.863
	RF	11624	0.786	0.807	0.872	0.708	0.642	0.765	0.675
	RT	175	0.741	0.770	0.839	0.843	0.794	0.843	0.868
DS10	J48	45	0.691	0.715	0.785	0.794	0.776	0.785	0.802
	RF	10884	0.708	0.720	0.876	0.741	0.683	0.757	0.712
	RT	157	0.716	0.774	0.885	0.877	0.811	0.881	0.922
DS11	J48	51	0.682	0.731	0.783	0.792	0.757	0.788	0.792
	RF	10036	0.802	0.802	0.930	0.708	0.629	0.807	0.700
	RT	143	0.706	0.794	0.922	0.905	0.881	0.922	0.934
DS12	J48	15	0.617	0.617	0.624	0.624	0.575	0.624	0.624
	RF	10482	0.753	0.782	0.881	0.683	0.675	0.765	0.641
	RT	163	0.741	0.807	0.881	0.881	0.839	0.881	0.905

Table 7. Obtained f1-scores by IBk classifier considering the different number of nearest neighbors (k), data variant, partition generator, and distance functions (DF)

Dataset	P	F	DF	# of nearest neighbors (k)							
				1	3	5	7	9	11	13	15
DS04	J48	77	CH	0.905	0.818	0.741	0.657	0.608	0.589	0.563	0.531
			EU	0.905	0.773	0.716	0.641	0.654	0.633	0.624	0.593
DS06	J48	77	CH	0.905	0.818	0.741	0.657	0.608	0.589	0.563	0.531
			EU	0.905	0.773	0.716	0.641	0.654	0.633	0.624	0.593
DS07	RT	145	CH	0.946	0.753	0.622	0.542	0.542	0.542	0.542	0.510
			EU	0.926	0.770	0.712	0.734	0.669	0.672	0.627	0.607
DS08	RT	141	CH	0.963	0.841	0.616	0.561	0.542	0.542	0.542	0.510
			EU	0.914	0.790	0.716	0.673	0.678	0.694	0.695	0.699
DS11	RT	143	CH	0.955	0.855	0.681	0.659	0.629	0.560	0.525	0.503
			EU	0.905	0.819	0.737	0.700	0.691	0.678	0.666	0.669
DS12	RT	163	CH	0.926	0.753	0.672	0.582	0.542	0.532	0.525	0.503
			EU	0.881	0.770	0.704	0.654	0.650	0.675	0.650	0.587

In Table 6, the best f1 score value for each dataset is written in bold, and the best classification f1 score for the table is written in red. As seen in Table 6, creating data variants affects both partition generators and estimators. The number of generated features changes depending on the data variant and the way the estimator trained on transformed variants produce different results. Using RF as a partition generator paves the way to have a high number of new features in all cases compared to the other two methods (i.e., J48 and RT). Contrarily, J48 produces fewer features in all cases compared to the RF and RT. Classifiers are akin to producing slightly different results considering data variants. However, it seems that the RT estimator is often superior to other estimators in terms of f1-score.

In detail, it seems that using RF as a partition generator is not a good idea since it produces a high number of features which is problematic in terms of run time (i.e., the training time of estimators) compared to its peers (i.e., J48 and RT). The highest f1 scores are often obtained when both the partition generator and estimator are chosen to be RT algorithms, respectively. The highest results are obtained on the data variants DS07, DS08, and DS11 whose common property is that they do not include both gender and age information at the same time. In this step, the best f1-score among all cases is obtained as 0.938 when the data variant is DS08, the partition generator and estimator are RT, respectively.

Upon completion of the second step, we performed an additional experimental analysis on the cases where the IBk classifier produced the best or second-best f1 scores for the respective data variant in Table 5. In this third step, we selected the data variants DS04, DS06, DS07, DS08, DS11, and DS12 and selected the partition generator as the same as in the previous step such that better results are obtained with the respective partition generator. Then, we performed classification experiments by using two different distance functions namely Euclidean (EU) and Chebyshev (CH) for different values of k which stands for the number of nearest neighbors. The results of this step are given in Table 7, which makes it clear that apart from the DS04 and DS06 changing the distance function improves the performance by using the CH method. The highest results in all cases are obtained when the parameter k takes a value of 1. On the other hand, the best results are obtained as an f1-score of 0.963 by the IBk classifier employed with the CH distance function and this is the best of our all results obtained so far.

DISCUSSION

Dementia is one of the neurodegenerative diseases that cause the brain atrophy in elderly people. There are several brain regions held in dementia and one of that the frontal lobe³⁹. The frontal lobe represents more than a third of the entire human hemisphere and it is associated with the complex cognitive

functions and behaviors of life. Besides its conspicuous relative size, the frontal lobe is a unique pattern of connections, the frontal areas establish to communicate among themselves and with other regions of the brain⁸. Moreover, the corpus callosum is a topographically organized neural structure that is composed of the majority of the commissural fibers connecting the two cerebral hemispheres^{40, 41}. Morphological variability in the corpus callosum is often found in diseases such as Alzheimer's disease, depression, autism, and schizophrenia^{41, 42}.

For evaluating the changes in the brain, MRI is one of the most choice brain imaging techniques that have cognitive impairments patients⁴³. There are many approaches for evaluating brain atrophy in dementia and the researchers prefer to measure brain volume for atrophy however, measuring some distances is not usually done³. Therefore, we studied the frontal lobe morphometry with linear measurements using MRI in healthy people and subjects with dementia in our population and we also evaluated the effects of age and gender in this paper. We expect that these findings will be useful for clinicians in determining the morphology of brain atrophy. Moreover, these data could provide a guide for planning surgery and to avoid damage to brain structures in the frontal lobe.

In the present study it was demonstrated that the brain atrophy was related with age and some changes in all measurements were found according to decades, whereas the means of A, B, E, and F had no significant differences with age in healthy group. Additionally, some measurements were shown differences due to gender in both healthy and dementia group (except F, I in healthy and in dementia A, B, E, F and I) that males' mean values higher than females'. Several approaches have been planned for the lesions of the frontal lobe. Furthermore, in the anterior part of the frontal lobe, two main approaches could be made: subfrontal and anterior interhemispheric routes. The subfrontal route could be important for surgeons for the lesions in the anterior cranial fossa which are located above the diaphragma sella such as pituitary adenoma, craniopharyngioma, tumors of optic nerve and hypothalamus^{44, 45}. This way has some advantages like showing the tumor better and protecting the great vessels. However, there are also some disadvantages that epileptic seizures, anosmia, and venous infarction⁴⁴. During this approach, some structures including the corpus callosum or the anterior

commissure should be preserved. Our measurements of the distances A (54.38mm), C (34.73mm) and D (41.95mm) can be useful for subfrontal approaches for the surgeon for avoiding damage to these structures. Ardeshiri et al. (2006) examined frontal lobe and central region of brain in 53 German subjects (mean age of 38.5 years) and the mean values were reported as A 60.3±6.3 mm, C 37.1±5.4 mm, D 47.2±5.6 mm⁴⁴. Additionally, in a study including elderly Greek people, the mean value of C was reported as 32.5 ±3.6 mm⁴⁶. When we analyzed the literature findings, our values are found: lower than Germans in all values, higher than Greeks' as seen in the C value. These diversities may be explained by the fact that different ages, populations, number of subjects and individual differences.

Moreover, the anterior interhemispheric approach is preferred for some pathologies like aneurysms of the distal anterior cerebral artery, midline lesions, and tumors of the third ventricle⁴⁴. Distal anterior cerebral artery aneurysms confront the surgeon with some problems including the limited surgical corridor between the skull and the corpus callosum. Kawashima et al (2003) reported a surgical anatomical study and determined a surgical landmark named PC (pericallosal) point, the point at which a parallel line along the long axis of infracallosal part of the pericallosal artery to the callosomarginal artery crosses the forehead⁴⁷. This parallel line takes its way nearly parallel to the distance between anterior and posterior commissure line (F) and lies between it and parallel to the F through the anterior-most point of the genu of the corpus callosum (G). The AC-PC line (F) is most commonly used in brain axial imaging. There are several kinds of AC-PC line in the literature and the most common two line used is the Talairach AC-PC line and the Schaltenbrand AC-PC line. Schaltenbrand (2005) AC-PC line passes through the center of the AC and the center of the PC and we used this line in the present study⁴⁸⁻⁵⁰. Kawashima et al. (2003) and colleagues established the thickness of the genu of the corpus callosum (I) as 11.2 ±2.0 mm in cadavers, we found lower value in MR scans⁴⁷. Our further findings for the interhemispheric route are F (mean; 25.72mm), G (mean; 32.6mm), and H (mean; 58.93±3.33mm). These data can be helpful for the anterior interhemispheric approaches. Additionally, the distance between the frontal pole and tuberculum sella (E) (mean: 49.95mm) is useful for basal procedures.

For analyzing the size of the brain atrophy in people who have dementia and healthy people, we used linear measurements concerning the frontal lobe morphometry and central region morphometry. Measurements enabled us to estimate atrophic changes of the brain tissue regarding the frontal lobe morphometry by aging. To our knowledge, there are not many studies considering frontal lobe morphometry on dementia in the literature. Therefore, these linear measurements in this paper could be helpful for predicting the surgical anatomy and approach in healthy and dementia groups in our elderly population.

In this study, it is studied performing automatic detection of dementia cases by using ML techniques. For this purpose, a real-world but rather small dataset of 243 instances is used in which each instance vector is formed to include 11 attributes. Using these 11 original features some of them obtained from MRI images the best f1 score is obtained as a value of 0.625 since the number of features is low and their values could not help estimators to differentiate instances of two classes namely healthy and dementia.

Hence, a supervised filter that creates new features based on the membership of attributes to automatically discovered regions applied to the original data and its variants. This enabled us to improve our results with a moderate increase in the number of features especially when the partition generator is selected to be RT. The main reason behind the success of this filter is the fact that it is a supervised method and uses class information of instances while discovering partitions/regions. Using the estimator, partition generator, and data variant in the best case, it is possible to build and deploy an ML model to assist medical personnel in the decision process of dementia cases. This could easily be accomplished by providing a graphical user interface to users in such a way that a user will be able to select or enter 11 parameters of a patient and then learn the prediction of the ML model by clicking a “make a prediction” button. In this deployment case, the ML model will first take the parameters of the patient and then create a test instance to pass through a previously trained partition generator. Then, the generator will transform the test instance and give a previously trained estimator. At the final stage, the estimator will make a prediction for the test instance by producing an output of 1 (dementia) or 2 (healthy).

Limitations of the study was that there were several new methods which will give detailed information

such as volumetric measurements or 3D imaging methods. Also, there is not enough study analyzed relation with ML-based prediction of Dementia for frontal lobe and central brain region. For this reason, the comparison of the other studies’ results is limited. Further research is needed to prove this idea clearly

In conclusion, the data obtained in this paper will give important detailed knowledge and normative data for frontal lobe morphometry according to age and gender in healthy and dementia people in our population. The anatomical landmarks of this study will be crucial for the brain region and thus, the data could be useful for surgeons for planning surgical procedures and avoiding to damage the structures in this area. Subjects having dementia are sensitive to age related changes than healthy subjects. Also, only one parameter called as the distance from frontal pole to tuberculum sella (E) of dementia subjects were similar to healthy subjects. According to age-related changes of frontal lobe and central region of brain measurements, there were significant differences in all measurements in dementia subjects. The means of the measurements were found higher in males than in females. Additionally, ML based supervised methods that were trained on the collected data for detection of dementia showed that it is required to provide as many attributes and instances as possible to train an accurate estimator. However, if this is not possible, by creating new features based on the hidden patterns between attributes and instances we could increase the success of the estimators up to 96.3% f-score value.

Author Contributions: Concept/Design : MÖ, SP, ÖÇ, SAÖ; Data acquisition: SP, MT, SAÖ; Data analysis and interpretation: SP, PG, SAÖ, ÖÇ; Drafting manuscript: SP, MT; Critical revision of manuscript: SP, PG, SAÖ; Final approval and accountability: SP, MT, MÖ, ÖÇ, SAÖ, PG; Technical or material support: MÖ, SAÖ, SP; Supervision: PG, SAÖ, SP, MÖ; Securing funding (if available): n/a.

Ethical Approval: Ethical approval was obtained from the Cukurova University Faculty of Medicine Non-Interventional Clinical Research Ethics Committee with its decision dated 10.9.2021 and numbered 114/62.

Peer-review: Externally peer-reviewed.

Conflict of Interest: Authors declared no conflict of interest.

Financial Disclosure: Authors declared no financial support

REFERENCES

1. Sacuiu SF, Dementias. *Handb Clin Neurol*. 2016;138:123-151.
2. Sorbi S, Hort J, Erkinjuntti T, Fladby T, Gainotti G, Gurvit H et al. EFNS-ENS Guidelines on the diagnosis and management of disorders associated with dementia. *Eur J Neurol*. 2012;19:1159-79.

3. Álvarez-Linera Prado J, Jiménez-Huete A. Neuroimaging in dementia. Clinical-radiological correlation. *Radiologia (Engl Ed)*. 2019;61:66-81.
4. Tartaglia MC, Rosen HJ, Miller BL. Neuroimaging in dementia. *Neurotherapeutics*. 2011;8:82-92.
5. Shah H, Albanese E, Duggan C, Igor R, Kenneth ML, Carrillo MC et al. Research priorities to reduce the global burden of dementia by 2025. *Lancet Neurol*. 2016;15:1285-94.
6. Prince M, Albanese E, Guerchet M, Prina M. World alzheimer report 2014: Dementia and risk reduction. an analysis of protective and modifiable factors. 2014.
7. Frisoni GB, Prestia A, Rasser PE, Bonetti M, Thompson PM. In vivo mapping of incremental cortical atrophy from incipient to overt Alzheimer's disease. *J Neurol*. 2009;256:916-24.
8. Catani M. The anatomy of the human frontal lobe. *Handb Clin Neurol*. 2019;163:95-122.
9. Schoenemann PT, Sheehan MJ, Glotzer LD. Prefrontal white matter volume is disproportionately larger in humans than in other primates. *Nat Neurosci*. 2005;8:242-52.
10. Semendeferi K, Lu A, Schenker N, Damasio H. Humans and great apes share a large frontal cortex. *Nat Neurosci*. 2002;5:272-76.
11. Smaers JB, Schleicher A, Zilles K, Vinicius L. Frontal white matter volume is associated with brain enlargement and higher structural connectivity in anthropoid primates. *PLoS One*. 2010;5:e9123.
12. Scheltens P, Leys D, Barkhof F, Huglo D, Weinstein HC, Vermersch P et al. Atrophy of medial temporal lobes on MRI in "probable" Alzheimer's disease and normal ageing: diagnostic value and neuropsychological correlates. *J Neurol Neurosurg Psychiatry*. 1992;55:967-72.
13. Scheltens P, Pasquier F, Weerts JG, Barkhof F, Leys D. Qualitative assessment of cerebral atrophy on MRI: inter- and intra-observer reproducibility in dementia and normal aging. *Eur Neurol*. 1997;37:95-9.
14. Jordan MI, Mitchell TM. Machine learning: Trends, perspectives, and prospects. *Science*. 2015;349:255-60.
15. Kusiak, A. Feature transformation methods in data mining. *Electronics packaging manufacturing, IEEE Transactions on*. 2001;24:214-7.
16. Frank E, Pfahringer B. Propositionalisation of multi-instance data using random forests. In *Australasian Joint Conference on Artificial Intelligence*. Springer, Cham, December 2013;362-73.
17. Pal NR, Jain L. *Advanced techniques in data mining and knowledge discovery*. Springer, 2005.
18. Foulds JR. *Learning instance weights in multi-instance learning (Doctoral dissertation)*. The University of Waikato, 2008.
19. Dietterich TG, Lathrop RH, Lozano-Pérez T. Solving the multiple instance problem with axis-parallel rectangles. *Artificial intelligence*. 1997;89:31-40.
20. Zhou, Z.H. *Multi-instance learning: A survey*. Department of Computer Science & Technology, Nanjing University, Tech. Rep., 2004.
21. Tian Y, Hao W, Jin D, Chen G, Zou A. A review of latest multi-instance learning. In *2020 4th International Conference on Computer Science and Artificial Intelligence*, 2020;41-4.
22. Foulds J, Frank E. A review of multi-instance learning assumptions. *The knowledge engineering review*. 2010;25:1-25.
23. Wu J, Pan S, Zhu X, Zhang C, Wu X. Multi-instance learning with discriminative bag mapping. *IEEE Transactions on Knowledge and Data Engineering*. 2018;30:1065-15.
24. Huang S, Liu Z, Jin W, Mu Y. Bag dissimilarity regularized multi-instance learning. *Pattern Recognition*. 2022;126:108583.
25. Babenko B. *Multiple instance learning: algorithms and applications*. View Article PubMed/NCBI Google Scholar. 2008;1-19.
26. Weidmann N, Frank E, Pfahringer B. A two-level learning method for generalized multi-instance problems. In *European Conference on Machine Learning Springer, Berlin, Heidelberg*, 2003;468-11.
27. Khan A, Baharudin B, Lee LH, Khan K. A review of machine learning algorithms for text-documents classification. *Journal of advances in information technology*, 2010;1:4-16.
28. Coban O. *Attribute inference over real-world online social networks: a comprehensive privacy analysis (Doctoral dissertation)*. Adana, Cukurova University, 2021.
29. Zafarani R, Abbasi MA, Liu H. *Social media mining: an introduction*. Cambridge University Press, 2014.
30. Kibriya AM, Frank E, Pfahringer B, Holmes G. Multinomial naive bayes for text categorization revisited. In *Australasian Joint Conference on Artificial Intelligence Springer, Berlin, Heidelberg*, 2004;488-11.
31. Su J, Shirab JS, Matwin S. Large scale text classification using semisupervised multinomial naive bayes. In *ICML*, 2011.
32. Platt J. Using analytic QP and sparseness to speed training of support vector machines. *Advances in neural information processing systems*. 1998:11.
33. Aha DW, Kibler D, Albert MK. Instance-based learning algorithms. *Machine learning*. 1991;6:37-29.
34. Breiman L. Random forests. *Machine learning*, 2001;45:5-27.
35. Quinlan JR. *C4.5: Program for machine learning*. San Francisco, Morgan Kaufmann Publishers Inc, 1993.
36. Mahesh B. *Machine learning algorithms-a review*. *IJSR*. 2020;9:381-5.
37. Alpaydin E. *Introduction to machine learning*. MIT press, 2020.
38. Kohavi R. A study of cross-validation and bootstrap for accuracy estimation and model selection. *Ijcai*. 1995;14:1137-8.

39. Risacher SL, Saykin AJ. Neuroimaging in aging and neurologic diseases. *Handb Clin Neurol*. 2019;167:191-227.
40. Pandya DN, Seltzer B. Two hemispheres-one brain: functions of the corpus callosum. *Neurology and neurobiology*. 1986;17:16-2.
41. Salat D, Ward A, Kaye JA, Janowsky JS. Sex differences in the corpus callosum with aging. *Neurobiol Aging*. 1997;18:191-97.
42. Karakaş P, Koç Z, Koç F, Bozkır MG. Morphometric MRI evaluation of corpus callosum and ventricles in normal adults. *Neurol Res*. 2011;33:1044-49.
43. Filippi M, Agosta F, Barkhof F, Dubois B, Fox NC, Frisoni GB et al. EFNS task force: the use of neuroimaging in the diagnosis of dementia. *Eur J Neurol*. 2012;19:e131-1501.
44. Ardeshiri A, Ardeshiri A, Wenger E, Holtmannspötter M, Winkler PA. Surgery of the anterior part of the frontal lobe and of the central region: normative morphometric data based on magnetic resonance imaging. *Neurosurg Rev*. 2006;29:313-21.
45. Ono M, Ono M, Rhoton AL Jr, Barry M. Microsurgical anatomy of the region of the tentorial incisura. *J Neurosurg*. 1984;60:365-99.
46. Mourgela S, Anagnostopoulou S, Sakellaropoulos A, Gouliamos A. An MRI study of sex-and age-related differences in the dimensions of the corpus callosum and brain. *Neuroanatomy*. 2007;6:63-2.
47. Kawashima M, Matsushima T, Sasaki T. Surgical strategy for distal anterior cerebral artery aneurysms: microsurgical anatomy. *J Neurosurg*. 2003;99:517-25.
48. Schaltenbrand G. Atlas for stereotaxy of the human brain. Georg Thieme. 1977.
49. Nowinski WL. Modified Talairach landmarks. *Acta Neurochir (Wien)*. 2001;143:1045-57.
50. Otake S, Taoka T, Maeda M, Yuh WT. A guide to identification and selection of axial planes in magnetic resonance imaging of the brain. *Neuroradiol J*. 2018;31:336-44.